ENVIRONMENTAL RESEARCH
LETTERS

LETTER • OPEN ACCESS

A link between surface air temperature and extreme precipitation over Russia from station and reanalysis data

To cite this article: M A Aleshina *et al* 2021 *Environ. Res. Lett.* **16** 105004

View the article online for updates and enhancements.

ENVIRONMENTAL RESEARCH
LETTERS

CrossMark

OPEN ACCESS

RECEIVED
25 March 2021

REVISED
10 August 2021

ACCEPTED FOR PUBLICATION
11 August 2021

PUBLISHED
27 September 2021

LETTER

A link between surface air temperature and extreme precipitation over Russia from station and reanalysis data

M A Aleshina[1,2,*], V A Semenov[1,2] and A V Chernokulsky[2]

[1] Institute of Geography, Russian Academy of Sciences, Moscow, Russia
[2] A.M. Obukhov Institute of Atmospheric Physics, Russian Academy of Sciences, Moscow, Russia
[*] Author to whom any correspondence should be addressed.

E-mail: aleshina@igras.ru

Keywords: precipitation extremes, C–C relationship, precipitation-temperature scaling, meteorological station data, Russia, ERA5 reanalysis, convective and large-scale precipitation

Supplementary material for this article is available online

Abstract

Precipitation extremes are widely thought to intensify with global warming due to an exponential growth following the Clausius–Clapeyron (C–C) equation which links the atmosphere water vapor saturation pressure with air temperature. However, a number of recent studies based on station and reanalyzes data for the contemporary period showed that scaling rates between extreme precipitation and temperature strongly depend on temperature range, moisture availability, and a region of interest. Being performed for some regions, such estimates, however, lack for Northern Eurasia, where prominent temperature changes and rapid shift from large-scale to convective precipitation are observed. Here, we examine the scaling between daily precipitation extremes and surface air temperature (SAT) over Russia for 1966–2017 using meteorological station data and for 1979–2020 using ERA5 reanalysis. The precipitation-temperature relation is examined for total precipitation and, separately, for convective and large-scale precipitation types. In winter, we reveal a general increase in extreme precipitation of all precipitation types according to the C–C relationship. For the Russian Far East region, the stratiform precipitation extremes scale with SAT following even super C–C rates, about two times as fast as C–C. However, in summer we find a peak-like structure of the precipitation-temperature scaling, especially for the convective precipitation in the southern regions. Extreme precipitation reaches their peak values at the temperature range between 15 °C and 20 °C. At higher temperatures, the negative scaling prevails. Analyzed data show a pronounced decrease in relative humidity with increasing surface temperatures beyond the 15 °C–20 °C threshold. This indicates that moisture availability is the major factor for the peak-shaped relationship between extreme precipitation and temperature revealed by our analysis.

1. Introduction

The ongoing surface air temperature (SAT) increase can modify the hydrological cycle around the world (Trenberth 2011). According to meteorological stations data, there is a 1%–2% per century increase of precipitation total amount from the middle of the 20th century over the continents (Contractor *et al* 2021). A significant positive trend in mean precipitation was observed in high and mid-latitudes in the Northern Hemisphere with a concurrent decrease in low-latitude precipitation (Trenberth 2011). However, the daily extreme precipitation intensity tends to increase almost everywhere over land, even in regions where precipitation totals tend to decrease, which poses an increase of extreme precipitation (Semenov and Bengtsson 2002, Donat *et al* 2016). The response of precipitation extremes to the warming is one of the key issues associated with the climate change. Increasing precipitation intensities and the occurrence of heavy rain events could cause devastating flash floods and affect economies and societies (e.g. Meredith *et al* 2015a, Mokhov and Semenov 2016, Martinkova and Kysely 2020). A better understanding of extreme precipitation formation processes will improve their prediction and accuracy in climate model simulations (Sillmann *et al* 2017).

Evaluation of such processes, particularly the response of precipitation extremes to temperature increase, is especially important for Northern Eurasia where the observed temperature trends substantially exceed the global one. According to instrumental observations, the average annual temperature trend over Russia was 0.47 °C per decade for 1976–2019. Thus, it is 2.5 times larger than the global SAT trend for the same period (0.18 °C per decade) and more than 1.5 times larger than the global trends over all land areas (0.28 °C per decade) (Bardin *et al* 2020).

Temperature increase in Northern Eurasia is accompanied with an increase of occurrence of hydrological and meteorological hazards, which number has doubled in the past 25 years over Russia (Mokhov and Semenov 2016). Many of these phenomena are associated with precipitation regime changes. These changes include an increase of the annual total precipitation with a 2.2% per decade trend for 1976–2019 over Russia (Bardin *et al* 2020). Also, an increase of the frequency of precipitation extremes was found in all seasons in Russia in the last five decades (Zolina and Bulygina 2016, Zolotokrylin and Cherenkova 2018). According to the Coupled Model Intercomparison Project Phase 6 (CMIP6) model experiments, observed tendencies may intensify in the future, for example, slight increased risk of wet events was found in the Northern Eurasia (Vogel *et al* 2020). Furthermore, an extreme precipitation intensity amplification is combined with an increased duration of dry and wet spells (Zolina *et al* 2010), which could enhance threat of both droughts and flashfloods. Finally, a moderate increase in total precipitation for the last 50 years over Northern Eurasia is accompanied by a relatively strong growth of convective precipitation and a concurrent decrease in large-scale precipitation (Chernokulsky *et al* 2019). A link between these precipitation changes in Northern Eurasia and SAT increase is remains understudied.

Theoretically, changes in the water vapor saturation pressure of the atmosphere and, respectively, daily precipitation extremes in global climate can be consistent with the 7% increase per degree of warming given by the Clausius–Clapeyron (C–C) relation (Pall *et al* 2007, Trenberth 2011, Westra *et al* 2014). However, the observed rate of extreme daily precipitation intensity diverges from this relation. Various scaling relations of precipitation extremes on temperature have been obtained worldwide (Hardwick Jones *et al* 2010, Mishra *et al* 2012, Westra *et al* 2014). For example, several studies have shown that the extreme precipitation intensity can occur even faster than the increase in the moisture content of the atmosphere, which may be due to the intensification of convective processes (Haerter and Berg 2009, Moseley *et al* 2016). Often a scaling exceeds the C-C relation forming a so-called super-C-C scaling (Lenderink and van Meijgaard 2008, Lenderink *et al* 2017). However, an increase that is slower than C–C has also been reported based on meteorological stations and reanalyzes data and model simulations (Hardwick Jones *et al* 2010, Drobinski *et al* 2016, Wang *et al* 2018) for many regions including Europe (Drobinski *et al* 2016, Martinkova and Kysely 2020), Australia (Visser *et al* 2020), China (Wang *et al* 2018, Huang *et al* 2019), South Korea (Park and Min 2017) and USA (Mishra *et al* 2012). Time scale of precipitation, e.g. hourly, sub-daily, or daily, plays an important role in such analysis (Visser *et al* 2020). On average, daily intensities increase at a slower rate with temperature than hourly intensities (Lenderink and van Meijgaard 2008).

Variances of observed precipitation-temperature scaling from the C–C scaling have been interpreted by different reasons. For instance, the response below the C–C scaling was explained by a lack of moisture availability that leads to the relative humidity (RH) decrease with increasing temperatures (Hardwick Jones *et al* 2010). The negative scaling in a hot climate was explained by the limitations of temperature by the balance of latent and sensible heat (Roderick *et al* 2019). Dynamic processes through the regional moisture balance alteration (O'Gorman and Schneider 2009, Pfahl *et al* 2017), atmospheric front strengthening (Berry *et al* 2011, Hénin *et al* 2019), global atmospheric circulation changes, (e.g. Hadley cell widening and its intensity changing (Seidel *et al* 2008)) are capable of altering the precipitation characteristics and patterns on the regional scale. Aerosol concentration variations in the troposphere may also affect precipitation characteristics and their link to temperature changes (Toll *et al* 2019).

In general, such studies' methodology involves the analysis of the relationship between the mean SAT and the extreme precipitation intensity characteristics for different regions, seasons, or precipitation types. For Russia, however, extreme precipitation-temperature scaling was only considered as a part of the global scale study using reanalysis or remote sensing data (Utsumi *et al* 2011, Wasko *et al* 2016, Ali *et al* 2018).

This study aims to assess a form of dependence between daily extreme precipitation and temperature using Russian meteorological stations data and the ERA5 reanalysis for the recent decades. In addition to scaling analysis for daily total precipitation amounts, we also separately investigated the response of convective and large-scale precipitations to temperature increase. Such analysis could clarify whether precipitation-temperature connection depends on precipitation types, in other words, different precipitation formation processes.

2. Data and methods

We analyzed daily observations from 538 Russian meteorological stations, obtained from the Al-Russian Research Institute of Hydrometeorological Information—World Data Center (RIHMI-WDC) for the 1966–2017 period (Bulygina *et al* 2014). Data on temperature, precipitation and RH were used. We separately analyze scaling for showery (convective) and stratiform (large-scale) precipitation types. For simplicity, we further will use terms ‘convective’ and ‘large-scale’. Data for precipitation types were obtained in Chernokulsky *et al* (2018) and Chernokulsky *et al* (2019), where routine meteorological reports on present and past weather and cloud morphological types were used to divide total precipitation into convective and large-scale one. A similar but somewhat less sophisticated approach was realized for meteorological stations in Europe (Haerter and Berg 2009) and South Korea (Park and Min 2017). In addition to observations data, we used the ERA5 reanalysis for 1979–2020 (Hersbach *et al* 2020), in particularly, we utilized daily amounts of total, convective and large-scale precipitation as well as temperature and RH. Also, specific and RH at 2 m was calculated based on ERA5 datasets for 2 m temperature, dew point temperature, and surface pressure.

In this study, we followed the method by Hardwick Jones *et al* (2010) to determine the scaling type between the average temperature and its typical value of extreme daily precipitation amounts for different Russian regions and different seasons using meteorological stations and ERA5 data separately. The 95th percentile daily precipitation intensity (P95) using only the data for wet days defined as >0.1 mm was estimated as a function of the temperature for each station and each reanalysis grid cell following the framework (Hardwick Jones *et al* 2010). Within this framework, at each station and grid point, the precipitation amount on a wet day was paired with the daily mean temperature at 2 m above ground level (T_{m}). The data were then rated by increasing temperatures and placed into bins of equal width (each bin contains 200 pairs). We then estimated the 95th percentile of precipitation (P95) and the average temperature (T_{m}) for each temperature bin. It is of note that temperature range varies among bins. The typical temperature range for the bins is around 0.4 °C–0.6 °C, varying from 0.1 °C for the most frequent temperature (in particular place) to 6 °C for the extreme temperature values. This approach is preferred over using temperature bins of equal width since it ensures a reasonable number of events across all bins that is essential for accurate extreme precipitation estimate. The same method has been used in Hardwick Jones *et al* (2010) and Ali *et al* (2018).

In the next step, a linear regression of logarithm of P95 (log(P95)) on the T_{m} was fitted to determine the degree to which the values agree with the C–C scaling. Also, we used the quadratic regression as the different type of simple polynomial function to distinguish the possible nonlinear response of extreme precipitation to increasing temperature. As a result, four scaling types of log(P95) changes with an increase in T_{m} were discriminated: monotonous increase, monotonous decrease, peak-like quadratic functions with maximum or with minimum. Within the peak-like scaling, extreme precipitation increases (or decreases) with T_{m} up to a particular threshold (hereafter, called the peak-point temperature) and then decreases (or increases) with a further increase in T_{m} (thus, parabola opens downward or upward) (see figure S1 (available online at stacks.iop.org/ERL/16/105004/mmedia)).

We took into account only those stations that display statistically significant linear or quadratic scaling. For the linear regression, we used the Student’s t-test (with p-value less than 0.05). For regions where the extreme precipitation decreases only at the highest temperatures, both linear and quadratic regressions can significantly fit the observations. In that case, we choose the regression type with the least standard deviation. The second requirement for a quadratic approximation is that the peak-point temperature fits within the observed temperature range.

We should stress that the described method provides no strict reflection of the physical principles that determine extreme precipitation changes with increasing temperature but rather shows the dependence type between two variables for the particular temperature range. It also depends on the sample size; however, we did not quantitatively estimate such dependence but used the entire time series.

3. Results

According to the C–C relation, atmospheric water vapor saturation pressure growths exponentially with temperature. One may expect that a logarithm of extreme precipitation, that usually fall out at the RH conditions close to saturation, increase linearly with temperature. This concept can be evaluated from figure 1 where statistically significant linear trends of a log(P95) as a function of T_{m} are shown for different seasons. The trends are computed based on both station and ERA5 reanalysis data.

Trends in a 6% °C^{-1}–8% °C^{-1} range indicate a good agreement with the C–C relation (implying 7% °C^{-1} water vapor saturation pressure growth rate). As seen in figure 1, such an agreement is found only in very limited regions of Russia. Trend rate and direction are strongly dependent on a season. In winter (figures 1(a) and (b)), the extreme

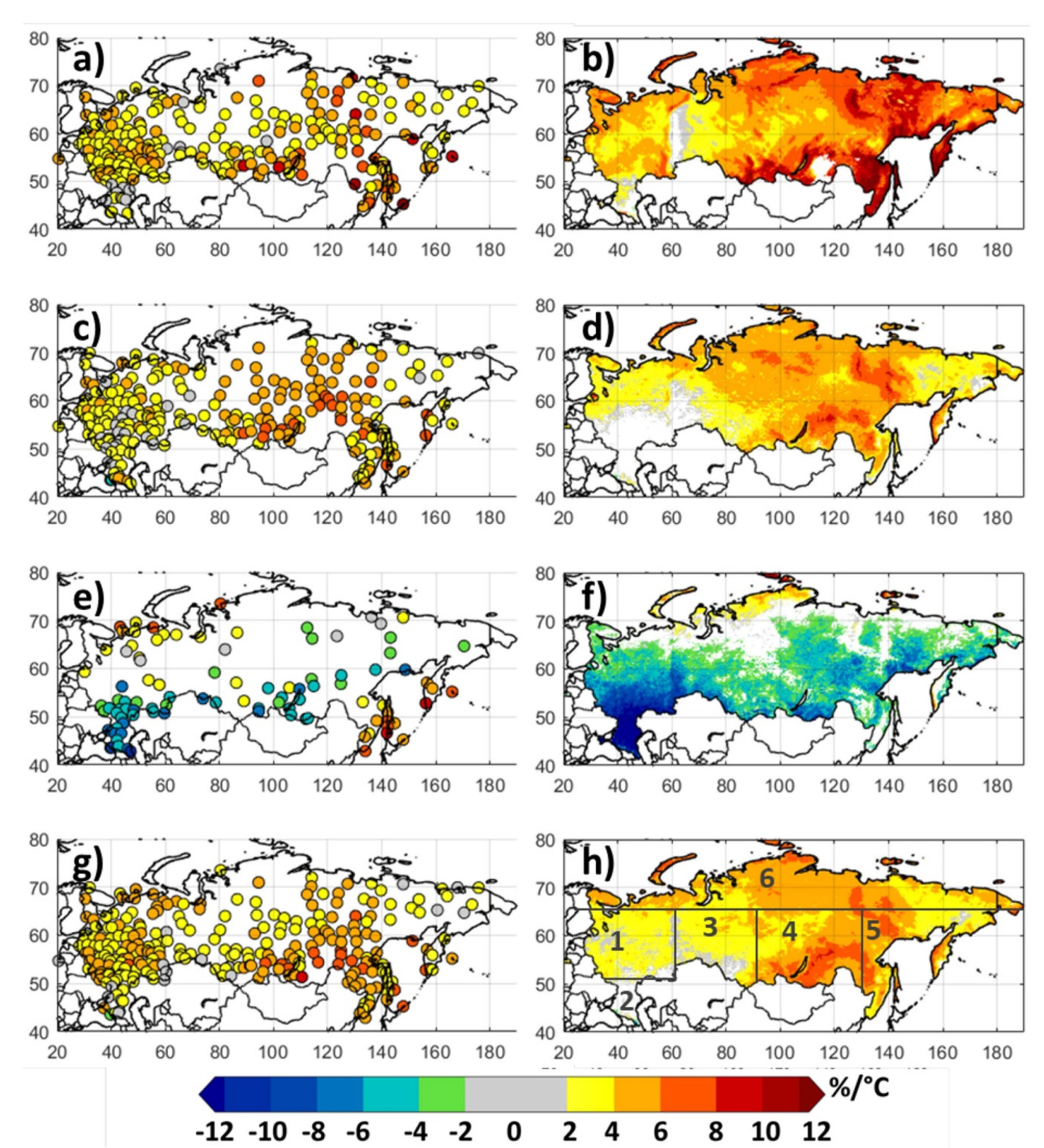

Figure 1. Linear trend (%/°C) of log(P95) as a function of T_m computed based on meteorological station data (a), (c), (e), (g) and the ERA5 reanalysis (b), (d), (f), (h) for winter (a), (b), spring (c), (d), summer (e), (f) and autumn (g), (h). Only statistically significant trends are shown (at 0.05 level). Gray lines on figure 1(h) show the scheme for dividing the entire analyzed region into six parts: 1—European Russia, 2—the southern part of European Russia, 3—western Siberia, 4—eastern Siberia, 5—the Russian Far East, 6—the Russian Arctic.

precipitation growth according to C–C relation is found in the Asian part of Russia (Taymyr Peninsula (the central part of region 6), northeast and south Siberia (region 4), and Far East of Russia (region 5) with a reasonable agreement between station and reanalysis data. For the most of Russian territory, extreme precipitation increases with temperature slower than expected from the C–C relation. An exception is relatively small regions in the Russian Far East (region 6) mostly in coastal areas, Sakhalin Island and the most southern parts of eastern Siberia (region 4) where the trends exceed the C–C rate by a factor of two or more. This is in agreement with a previous study (Chernokulsky *et al* 2019) on precipitation intensity trends over Russian territory in the last 40 years that revealed the strongest precipitation increase in the south of the Russian Far East (region 6). Such an increase implied a 13.8% daily precipitation intensity growth with 1 °C warming. The increase was mainly due to convective precipitation. In summer, except for some northern regions, there is a distinct decrease of extreme precipitation intensity with growing temperature. This tendency amplifies in southern regions and reaches $-12\ldots-14\%\ ^{\circ}\mathrm{C}^{-1}$ in south of European Russia (region 2). In spring and autumn, the trends are in general similar to the winter

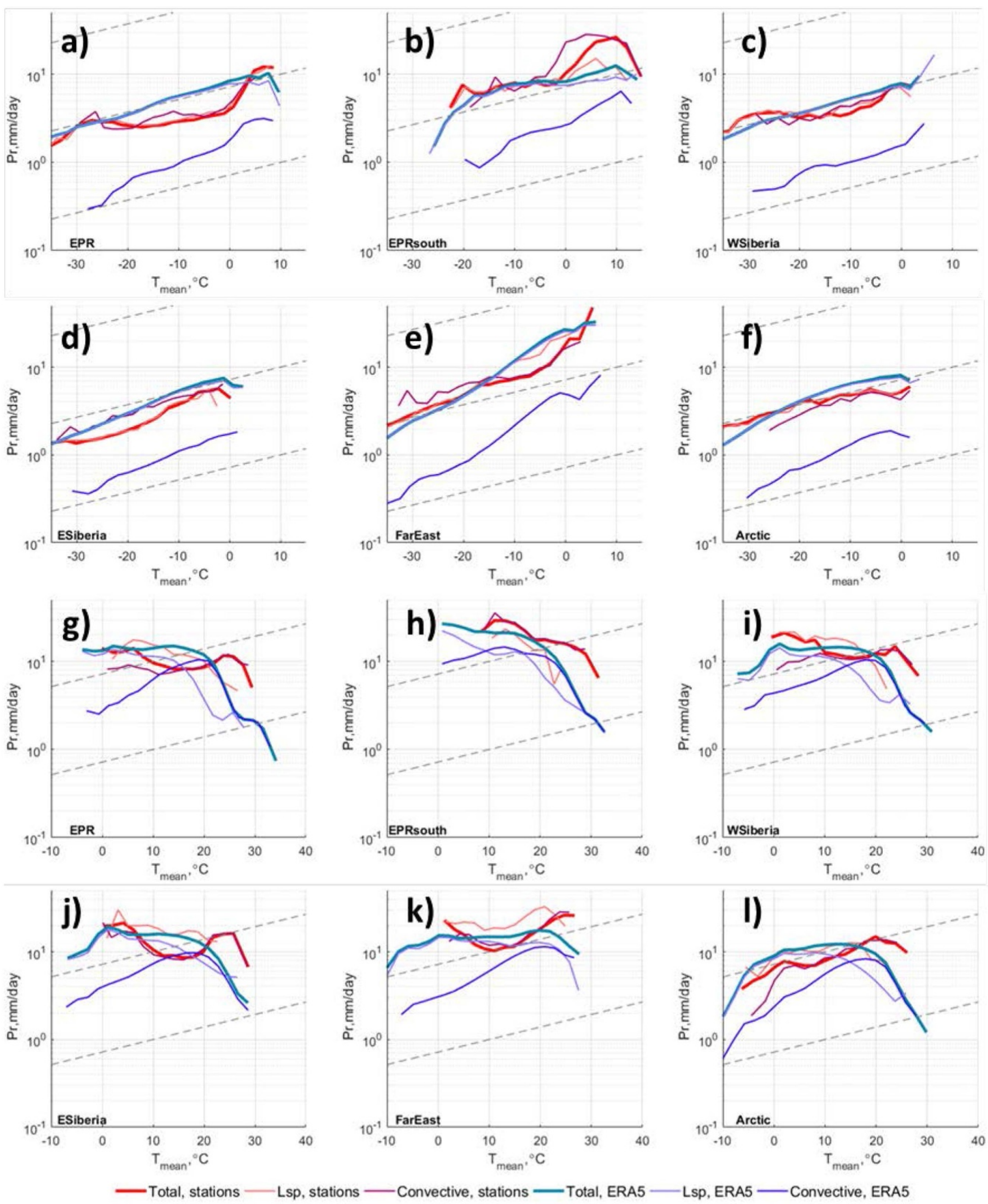

Figure 2. Values of the 95th percentile of total daily precipitation, large-scale precipitation and convective precipitation as a function of the daily mean SAT in winter (a)–(f) and summer (g)–(l) as derived from meteorological station data (red lines) and ERA5 reanalysis (blue lines) for: European Russia (a), (g), south of European Russia (b), (h), western Siberia (c), (i), eastern Siberia (d), (j), the Far East (e), (k) and the Russian Arctic (f), (l). Dashed lines show a slope corresponding to the C–C relation (about 7%/°C).

ones. Extreme precipitation increases by 6% °C^{-1}–8% °C^{-1} only in southern part of eastern Siberia (region 4), and some restricted areas in the north-eastern Siberia (east of Sakha Republic). The rest of Russian territory is covered by weaker trends that do not exceed 3% °C^{-1} in European part of Russia (region 1) and became statistically insignificant in the southern part of the latter.

Reanalysis data in general reproduce the regional and seasonal peculiarities of the log(P95)–T_m relation obtained from meteorological station data. A noticeable distinction is much smaller areas with statistically insignificant trends in summer and spring.

Dependencies of extreme precipitation on SAT are illustrated in figure 2 for six parts of Russian territory (shown by gray lines in figure 1(h)). These regions were chosen to roughly represent the revealed major regional peculiarities of the linear trends depicted in figure 1. For the regional assessment, we combined all initial datasets into a single array related to a particular region, and then applied the scaling procedure.

The dependencies at figure 2 are shown for total daily extreme precipitation, and, separately, for daily convective and large-scale precipitation diagnosed from station data and taken from reanalysis dataset for winter and summer.

In winter (figures 2(a)–(f)), there is a general monotonic increase of extreme precipitation with temperature that well fits to the C–C relation in European Russia (region 1), western and eastern Siberia (regions 3 and 4), and in the Arctic (region 6). In the Russian Far East (region 5), as it was discussed before, there is a super C–C extreme precipitation increase. Convective precipitation in winter is a rare event. Therefore, only few stations in southern Russia (region 2) provided a statistically significant connection to deduce a relationship with temperature, which appeared to be positive and close to linear (i.e. the C–C in the logarithm scale). Also, convective precipitation deduced from reanalysis data are considerably less intense that estimated from station data.

At the same time, although a linear relation of the logarithm of daily precipitation extremes on temperature in general proves to be a reasonable approximation for winter season, one can often see considerable deviations from a linear trend. This is particularly evident for European Russia (region 1) and its southern regions (figures 2(a) and (b)).

In summer, a dependence of extreme precipitation intensity on temperature is, in general, strongly non-linear. Extreme precipitation increases with growing temperature until about 10 °C –15 °C, then the increase ceases and it may start to decrease. In some regions, e.g. in the southern part of European Russia (region 1), there is a monotonic decrease of extreme precipitation intensity with temperature increase in summer.

The linear log(P95)-T_m approximation works generally well only in winter and with some noticeable exceptions, whereas other seasons very often demonstrate strongly non-linear log(P95)-T_m dependence. To distinguish between linear and non-linear types of approximations, a test of a better fit (in terms of root mean square error) for the linear or parabolic approximations was performed using station and reanalysis data for different seasons (see 'Data and methods' section and figure 3). The test revealed that upward parabola provides a better approximation for log(P95)-T_m dependence for all seasons except winter when linear trend shows in general a better fit (figure 3). The linear trend in winter is usually less than the C–C rate being in 4%–6%/°C range, corresponds to C–C in southern Siberia and has super C–C values in the Russian Far East maritime regions (region 5). In summer in the majority of regions, extreme precipitation increases with temperature until a certain threshold and decreased beyond it. Only at a few stations (and reanalysis grid cells) a better approximation corresponds to a downward parabola or a negative linear trend (figure 3).

A general feature for all seasons is underestimation of extreme precipitation (mostly of convective origin) in ERA5 reanalysis in comparison to those derived from station data. On the one hand, this may be related to a grid-cell representation of precipitation in atmospheric models used in reanalysis products with spatial resolution still too coarse to resolve convective scale processes (Volosciuk *et al* 2015, Meredith *et al* 2015b). On the other hand, a difference in convective precipitation as defined in reanalysis output and diagnosed from station data using observation of cloudiness and weather features (Chernokulsky *et al* 2019) may play a role.

Several studies (e.g. Bao *et al* 2017, Barbero *et al* 2018) addressed a question of possible surface temperature cooling during extreme precipitation events due to downdrafts or cloudiness cooling effect. This phenomenon may reassign high intensity precipitation events to lower local temperatures and contribute to the parabolic log(P95)-T_m form. To estimate the importance of this factor, probability density functions (PDFs) of temperature differences in a day of extreme precipitation and in a day before were computed (figure S2). In winter, the mean of the PDF is positive implying a warming by 2 °C–3 °C on average in the day of extreme precipitation compared to the preceding day for the majority of the analyzed regions. PDFs are generally skewed strongly positive implying increasing probability of stronger warming events accompanying extreme precipitation. In summer, on contrary, temperature decreases in the day of the event but the average cooling is smaller, about 1 °C–1.5 °C. However, given a wide range of temperature differences of both positive and negative signs compared to the relatively weak warming/cooling in winter/summer, we speculate that the temperature change effect may not be a major factor for bending log(P95)-T_m curve at high temperature especially in summer.

Another feasible hypothesis that may explain the decrease of extreme precipitation with temperature higher than 15 °C–20 °C in many Russian regions in summer is an impact of changes in RH as an indicator of moisture content and, partly, static stability of the atmosphere. The dependence of RH on SAT for the events of extreme precipitation ($P > 95$th percentile) for the same regions as depicted in figure 2 in winter and summer is shown in figure 4.

In winter, the RH during precipitation events is in the range of 70%–80% for low temperatures (below −20 °C) and monotonically increases (with increasing temperature) exceeding 90% when temperature is approaching zero. Such a behavior is valid in winter for all regions except for the south of European Russia (figure 4(c)). In this region, winter temperatures are usually positive and extreme precipitation falls in conditions of 90%–100% RH. For negative

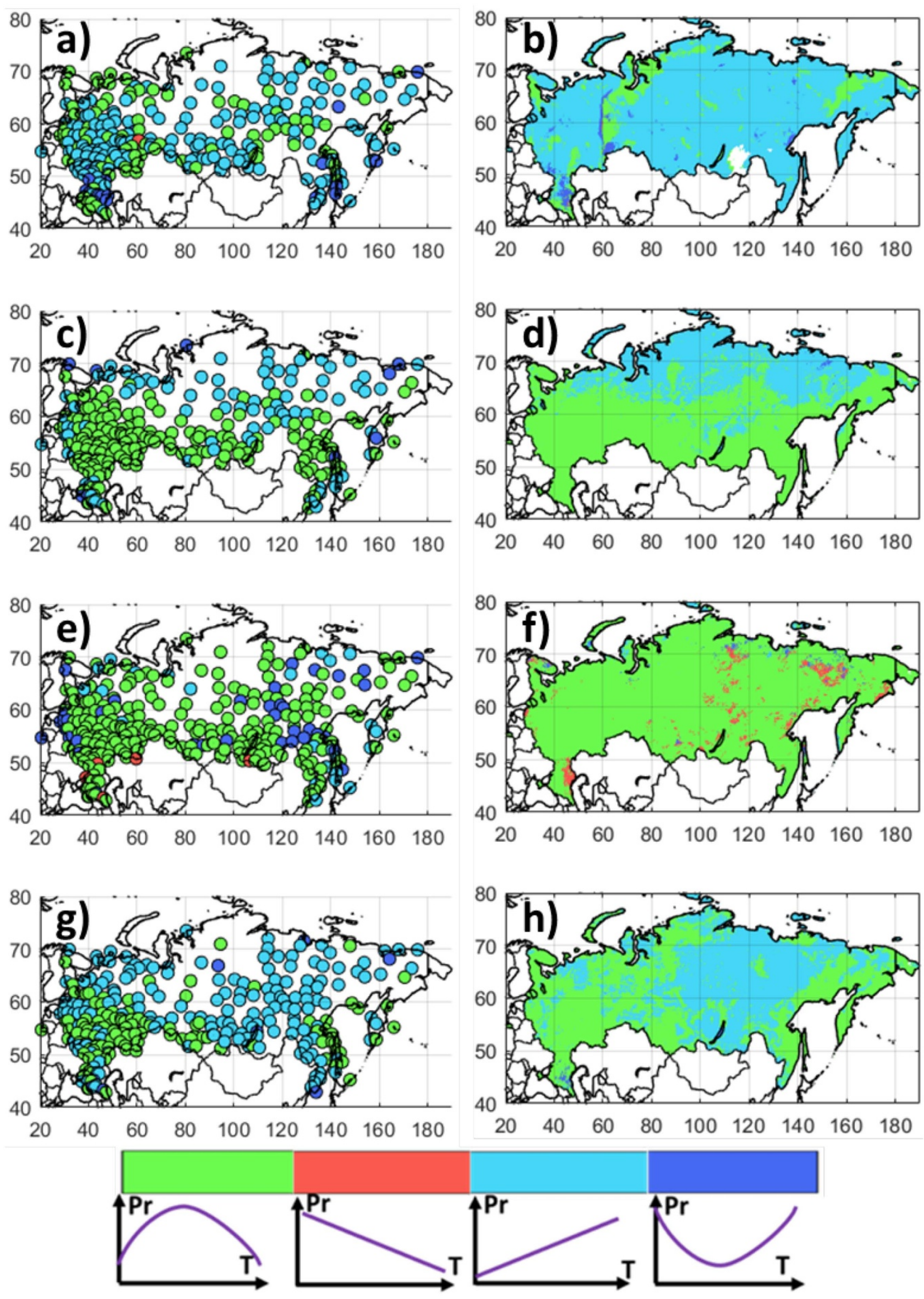

Figure 3. Types of scaling between temperature and extreme precipitation based on meteorological station data (a), (c), (e), (g) and the ERA5 reanalysis (b), (d), (f), (h) for winter (a), (b), spring (c), (d), summer (e), (f), and autumn (g), (h).

temperatures, RH grows as in the other regions but when temperature exceeds zero, RH starts to decrease thus making an upward parabolic dependence similar to the log(P95)-T_m behavior deduced form station data (figure 2(b)) in this region.

In summer, despite a wide range of RH values for the same temperature intervals, there is a clear tendency of RH decrease with temperature exceeding 15 °C–20 °C threshold that is also accompanied by extreme precipitation growth.

The reanalysis data produce in general similar results (see figure S3). Noticeable difference is wide range of RH values (likely due to a larger sampling) and a tendency of RH-T curve to bend

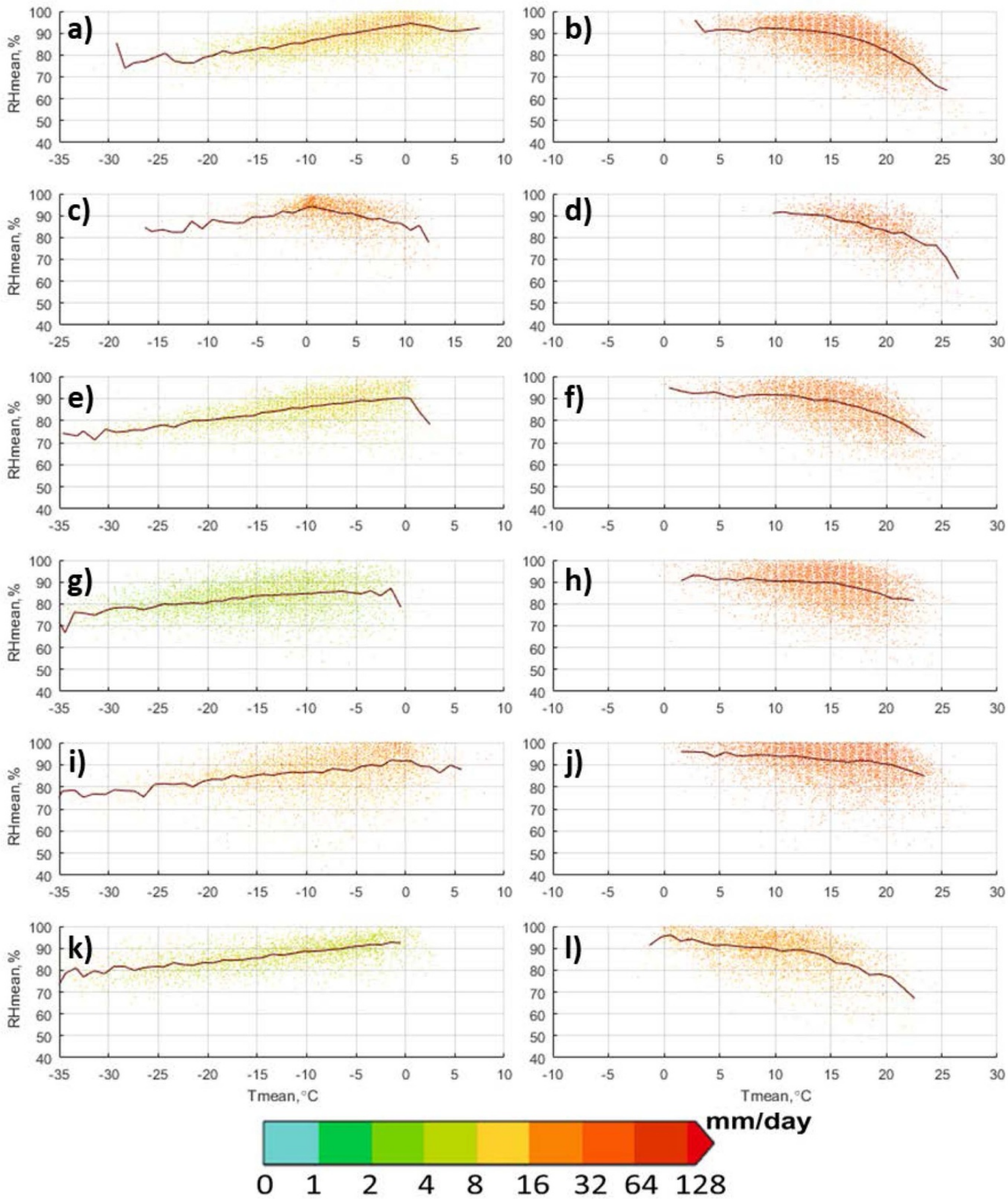

Figure 4. RH at 2 m (%) for the events of extreme precipitation as a function of temperature in winter (a), (c), (e), (g), (i), (k) and summer (b), (d), (f), (h), (j), (l) based on meteorological stations' data in: European Russia (a), (b), south of European Russia (c), (d), western Siberia (e), (f), eastern Siberia (g), (h), the Far East (i), (j), and the Russian Arctic (k), (l). Precipitation intensity (mm/day) is shown by color.

down in winter when temperature close or above zero. We performed the same procedure for large-scale and convective precipitation, separately (see S4–S7). In summer, decrease of RH with temperature increase is more pronounced for convective precipitation, both for meteorological stations and ERA5 data.

Thus, the observed decrease of RH with temperature in the events of extreme precipitation may at least partly explain the corresponding decrease of extreme precipitation at high temperatures. It can be also noted that the temperature threshold at which RH starts to bend down rather well corresponds to the extremum of upward parabola used to approximate log(P95)-T_m relation (figure 2). This result indicates that moisture deficit under increased temperature conditions caused by dynamical factors can be an important factor impacting extreme precipitation change under global warming. In particular, the northward shift of the downward branch of Hadley circulation in the last decades may explain the absence of precipitation intensity increase at the Caucasian Black Sea coast despite the strong SAT and sea surface temperature increase (Aleshina et al 2018).

4. Discussion and conclusions

A large number of extreme precipitation events have led to substantial economic and social consequences in Russia in recent decades (e.g. Meredith *et al* 2015a, Mokhov and Semenov 2016, Zolotokrylin and Cherenkova 2018). Understanding the processes determining extreme precipitation is important for more accurate weather forecasts and climate projections. This, in turn, can minimize the potential risks from extreme events in the changing climate (Sillmann *et al* 2017).

In this study, the relationship between the 95th percentile daily precipitation intensity and SAT was investigated over Russia for more than the last 50 years using meteorological stations data and more than 40 years using reanalysis data. Link of two precipitation types, i.e. convective and large-scale, on SAT increase were analyzed as well.

Recent studies have shown that precipitation extremes increase monotonically with temperature at high latitudes. In mid-latitudes, precipitation extremes increase at lower temperature and decrease at higher temperature, forming a peak like structure; while in tropics, they show a monotonic increase with temperature (Utsumi *et al* 2011, Ali *et al* 2018). Our analysis confirmed previous findings and revealed that scaling rates of extreme precipitation with temperature significantly deviate from the C-C rate depending on season, region, and precipitation type.

In winter, the precipitation increases according to C–C relation at the rates of 6% $°C^{-1}$–8% $°C^{-1}$ only in a few regions. The majority of areas are characterized by a weaker, but still positive, response to temperature increase. However, the precipitation increases two times faster than expected in the Far East and southern part of eastern Siberia.

In summer, the simultaneous increase of temperature and extreme precipitation occurs up to the temperature thresholds around 15 °C–20 °C. As temperature continues to rise over this threshold, precipitation starts to decrease. Negative scaling rates have been attributed to a decrease in RH at higher temperatures (Hardwick Jones *et al* 2010, Gao *et al* 2020). Our analysis of RH on wet days showed high importance of this factor for the extreme precipitation events. In summer, there is a clear tendency of RH decrease with temperature exceeding 15 °C–20 °C threshold that is also accompanied by extreme precipitation growth. In our work, we used the RH as a characteristic of moisture availability. The similar approach was implemented in Hardwick Jones *et al* (2010). However, there are other possible methods to evaluate moisture availability, for instance, using specific humidity or dew point temperature (Lenderink *et al* 2018, Huang *et al* 2019, Fowler *et al* 2021). Corresponding results provide compelling evidence that it may not be straightforward to predict the precipitation response from the temperature scaling. The choosing of the most informative moisture characteristics to evaluate precipitation scaling dependence on moisture availability deserves further investigations.

The ERA5 reanalysis data successfully reproduce the main regional and seasonal features of the log(P95)-T_m relation obtained from the station data. The reanalysis shows a robust negative scaling in the southern regions in summer, while there is a small number of meteorological stations with significant connections. However, the reanalysis tends to underestimate extreme precipitation (mostly those of convective type) for all seasons. This is primarily related to the gridded data representation in atmospheric models and reanalyzes that leads lower precipitation intensities (Volosciuk *et al* 2015). Furthermore, different precipitation separation technologies apply for reanalysis and meteorological station data, leading to observed differences in the contribution of convective precipitation (Chernokulsky *et al* 2019).

The different response in winter and summer is related to different temperature ranges and also indicates that contribution of various dynamical and thermo-dynamical factors may change with increasing temperatures. In winter, the saturation water vapor pressure is relatively small in the cooler conditions, and less vapor is needed to saturate the air. Excessive latent heat release that increases upward motions in clouds leading to enhance moisture convergence and change in rainfall type from stratiform (large scale frontal precipitation) to high intensity convective have been argued as possible causes for Super C-C scaling (Haerter and Berg 2009, Lenderink et al 2017). The poleward shift of storm tracks (Seidel *et al* 2008) especially pronounced in winter, leads to a decrease in large-scale precipitation in southern regions of Northern Eurasia and to an increase in central and northern regions. For example, changes in circulation patterns for moisture transport were identified as a main reason for wintertime extreme precipitation events over South China (Huang *et al* 2018).

In summer, when the temperature is higher, a larger amount of water in the air is needed to start condensation and cloud formation. Also, deviations from the CC ratio can occur due to the influence of large-scale and regional atmospheric circulation features such as Hadley cell widening (Seidel *et al* 2008), monsoon dynamics (Pfahl *et al* 2017), mountain circulations, effects of orography (Drobinski *et al* 2016) and land use. Furthermore, local moisture sources (large lakes, reservoirs, swamps), and the aerosol concentrations could be an additional source of latent heat flux and cloud alteration.

Thermodynamic, dynamic, and microphysical processes can differently influence different types of extreme precipitation. The share of extreme convective precipitation in total precipitation has increased in Russia in the last 50 years (Chernokulsky *et al* 2019).

Intensification of convective processes over Northern Eurasia is also manifested in increase of convective clouds (Chernokulsky and Esau 2019), major convective-related windthrow (Shikhov *et al* 2020), convective initiating environments (Chernokulsky *et al* 2017). However, occurrence of convective inhibiting environments has also increased, at least over European Russia (Taszarek *et al* 2021), which may be associated with sea surface warming (Meredith *et al* 2015a). No estimates for mutual changes of convective inhibiting and convective initiating environments have been carried out for other Russian regions though. Such estimates, accompanied with assessments of relative role of moisture availability and dynamical processes, may help to clarify the character of a link between extreme SAT and extreme precipitation.

Data availability statement

The data that support the findings of this study are available upon reasonable request from the authors.

Acknowledgments

This study was supported by the Russian Science Foundation through a Project No. 19-17-00242. Data processing was supported by the Russian Foundation for Basic Research (Projects No. 20-55-14003, 20-35-70044). The analysis of link between precipitation and humidity was supported by Ministry of Science and Higher Education of the Russian Federation (Agreement No. 075-15-2021-577).

ORCID iDs

M A Aleshina https://orcid.org/0000-0001-8416-7657
V A Semenov https://orcid.org/0000-0001-7632-7921
A V Chernokulsky https://orcid.org/0000-0003-3635-6263

References

Aleshina M A, Toropov P A and Semenov V A 2018 Temperature and humidity regime changes on the Black Sea Coast in 1982—2014 *Russian Meteorol. Hydrol.* **43** 235–44

Ali H, Fowler H J and Mishra V 2018 Global observational evidence of strong linkage between dew point temperature and precipitation extremes *Geophys. Res. Lett.* **45** 12–320

Bao J, Sherwood S C, Alexander L V and Evans J P 2017 Future increases in extreme precipitation exceed observed scaling rates *Nat. Clim. Change* **7** 128–32

Barbero R, Westra S, Lenderink G and Fowler H J 2018 Temperature-extreme precipitation scaling: a two-way causality? *Int. J. Climatol.* **38** e1274–79

Bardin M Y, Ran'kova E Y, Platova T V, Samokhina O F and Korneva I A 2020 Modern surface climate change as inferred from routine climate monitoring data *Russian Meteorol. Hydrol.* **45** 317–29

Berry G, Reeder M J and Jakob C 2011 A global climatology of atmospheric fronts *Geophys. Res. Lett.* **38** 4

Bulygina O N, Veselov V M, Razuvaev V N and Aleksandrova T M 2014 *Database State Regist. Certif.*) №2014620942 (http://meteo.ru/data/162-temperature-precipitation)

Chernokulsky A V, Kozlov F A, Zolina O G, Bulygina O N and Semenov V A 2018 Climatology of precipitation of different genesis in Northern Eurasia *Russian Meteorol. Hydrol.* **43** 425–35

Chernokulsky A V, Kurgansky M V and Mokhov I I 2017 Analysis of changes in tornadogenesis conditions over northern Eurasia based on a simple index of atmospheric convective instability *Doklady Earth Sci.* **477** 1504–9

Chernokulsky A and Esau I 2019 Cloud cover and cloud types in the Eurasian Arctic in 1936–2012 *Int. J. Climatol.* **39** 5771–90

Chernokulsky A, Kozlov F, Zolina O, Bulygina O, Mokhov I I and Semenov V A 2019a Observed changes in convective and stratiform precipitation in Northern Eurasia over the last five decades *Environ. Res. Lett.* **14** 045001

Contractor S, Donat M G and Alexander L V 2021 Changes in observed daily precipitation over global land areas since 1950 *J. Clim.* **34** 3–19

Donat M G, Lowry A L, Alexander L V, O'Gorman P A and Maher N 2016 More extreme precipitation in the world's dry and wet regions *Nat. Clim. Change* **6** 508–13

Drobinski P, Alonzo B, Bastin S, Silva N D and Muller C 2016 Scaling of precipitation extremes with temperature in the French Mediterranean region: what explains the hook shape? *J. Geophys. Res.: Atmos.* **121** 3100–19

Fowler H J *et al* 2021 Anthropogenic intensification of short-duration rainfall extremes *Nat. Rev. Earth Environ.* **2** 107–22

Gao X, Guo M, Yang Z, Zhu Q, Xu Z and Gao K 2020 Temperature dependence of extreme precipitation over mainland China *J. Hydrol.* **583** 124595

Haerter J O and Berg P 2009 Unexpected rise in extreme precipitation caused by a shift in rain type? *Nat. Geosci.* **2** 372–3

Hardwick Jones R, Westra S and Sharma A 2010 Observed relationships between extreme sub-daily precipitation, surface temperature, and relative humidity *Geophys. Res. Lett.* **37** L22805

Hénin R, Ramos A M, Schemm S, Gouveia C M and Liberato M L 2019 Assigning precipitation to mid-latitudes fronts on sub-daily scales in the North Atlantic and European sector: climatology and trends *Int. J. Climatol.* **39** 317–30

Hersbach H *et al* 2020 The ERA5 global reanalysis *Q. J. R. Meteorol. Soc.* **146** 1999–2049

Huang D, Yan P, Xiao X, Zhu J, Tang X, Huang A and Cheng J 2019 The tri-pole relation among daily mean temperature, atmospheric moisture and precipitation intensity over China *Glob. Planet Change* **179** 1–9

Huang W, He X, Yang Z, Qiu T, Wright J S, Wang B and Lin D 2018 Moisture sources for wintertime extreme precipitation events over South China during 1979–2013 *J. Geophys. Res.: Atmos.* **123** 6690–712

Lenderink G, Barbero R, Loriaux J M and Fowler H J 2017 Super-Clausius–Clapeyron scaling of extreme hourly convective precipitation and its relation to large-scale atmospheric conditions *J. Clim.* **30** 6037–52

Lenderink G, Barbero R, Westra S and Fowler H J 2018 Reply to comments on 'Temperature-extreme precipitation scaling: a two-way causality?' *Int. J. Climatol.* **38** 4664–6

Lenderink G and van Meijgaard E 2008 Increase in hourly precipitation extremes beyond expectations from temperature changes *Nat. Geosci.* **1** 511–4

Martinkova M and Kysely J 2020 Overview of observed Clausius-Clapeyron scaling of extreme precipitation in midlatitudes *Atmosphere* **11** 786

Meredith E P, Maraun D, Semenov V A and Park W 2015b Evidence for added value of convection-permitting models for studying changes in extreme precipitation *J. Geophys. Res.: Atmos.* **120** 12500–13

Meredith E P, Semenov V A, Maraun D, Park W and Chernokulsky A V 2015a Crucial role of Black Sea warming in amplifying the 2012 Krymsk precipitation extreme *Nat. Geosci.* **8** 615–9
Mishra V, Wallace J M and Lettenmaier D P 2012 Relationship between hourly extreme precipitation and local air temperature in the United States *Geophys. Res. Lett.* **39** L16403
Mokhov I I and Semenov V A 2016 Weather and climate anomalies in Russian regions related to global climate change *Russian Meteorol. Hydrol.* **41** 84–92
Moseley C, Hohenegger C, Berg P and Haerter J O 2016 Intensification of convective extremes driven by cloud–cloud interaction *Nat. Geosci.* **9** 748–52
O'Gorman P A and Schneider T 2009 Scaling of precipitation extremes over a wide range of climates simulated with an idealized GCM *J. Clim.* **22** 5676–85
Pall P, Allen M R and Stone D A 2007 Testing the Clausius–Clapeyron constraint on changes in extreme precipitation under CO_2 warming *Clim. Dyn.* **28** 351–63
Park I H and Min S K 2017 Role of convective precipitation in the relationship between subdaily extreme precipitation and temperature *J. Clim.* **30** 9527–37
Pfahl S, O'Gorman P A and Fischer E M 2017 Understanding the regional pattern of projected future changes in extreme precipitation *Nat. Clim. Change* **7** 423–7
Roderick T P, Wasko C and Sharma A 2019 Atmospheric moisture measurements explain increases in tropical rainfall extremes *Geophys. Res. Lett.* **46** 1375–82
Seidel D J, Fu Q, Randel W J and Reichler T J 2008 Widening of the tropical belt in a changing climate *Nat. Geosci.* **1** 21–24
Semenov V A and Bengtsson L 2002 Secular trends in daily precipitation characteristics: greenhouse gas simulation with a coupled AOGCM *Clim. Dyn.* **19** 123–40
Shikhov A N, Chernokulsky A V, Azhigov I O and Semakina A V 2020 A satellite-derived database for stand-replacing windthrows in boreal forests of the European Russia in 1986–2017 *Earth Syst. Sci. Data Discuss.* **12** 3489–513
Sillmann J, Thorarinsdottir T, Keenlyside N, Schaller N, Alexander L V, Hegerl G, Seneviratne S I, Vautard R, Zhang X and Zwiers F W 2017 Understanding, modeling and predicting weather and climate extremes: challenges and opportunities *Weather Clim. Extremes* **18** 65–74
Taszarek M, Allen J T, Brooks H E, Pilguj N and Czernecki B 2021 Differing trends in United States and European severe thunderstorm environments in a warming climate *Bull. Am. Meteorol. Soc.* **102** E296–322
Toll V, Christensen M, Quaas J and Bellouin N 2019 Weak average liquid-cloud-water response to anthropogenic aerosols *Nature* **572** 51–55
Trenberth K E 2011 Changes in precipitation with climate change *Clim. Res.* **47** 123–38
Utsumi N, Seto S, Kanae S, Maeda E E and Oki T 2011 Does higher surface temperature intensify extreme precipitation? *Geophys. Res. Lett.* **38** L16708
Visser J B, Wasko C, Sharma A and Nathan R 2020 Resolving inconsistencies in extreme precipitation-temperature sensitivities *Geophys. Res. Lett.* **47** e2020GL089723
Vogel M M, Hauser M and Seneviratne S I 2020 Projected changes in hot, dry and wet extreme events' clusters in CMIP6 multi-model ensemble *Environ. Res. Lett.* **15** 094021
Volosciuk C, Maraun D, Semenov V A and Park W 2015 Extreme precipitation in an atmosphere general circulation model: impact of horizontal and vertical model resolutions *J. Clim.* **28** 1184–205
Wang H, Sun F and Liu W 2018 The dependence of daily and hourly precipitation extremes on temperature and atmospheric humidity over China *J. Clim.* **31** 8931–44
Wasko C, Parinussa R M and Sharma A 2016 A quasi-global assessment of changes in remotely sensed rainfall extremes with temperature *Geophys. Res. Lett.* **43** 12–659
Westra S, Fowler H J, Evans J P, Alexander L V, Berg P, Johnson F, Kendon E J, Lenderink N and Roberts N M 2014 Future changes to the intensity and frequency of short-duration extreme rainfall *Rev. Geophys.* **52** 522–55
Zolina O and Bulygina O 2016 Current climatic variability of extreme precipitation in Russia *Fundam. Appl. Climatol.* **1** 84–103
Zolina O, Simmer C, Gulev S K and Kollet S 2010 Changing structure of European precipitation: longer wet periods leading to more abundant rainfalls *Geophys. Res. Lett.* **37** L06704
Zolotokrylin A and Cherenkova E 2018 Seasonal changes in precipitation extremes in Russia for the last several decades and their impact on vital activities of the human population *Geogr. Environ. Sustain.* **10** 69–82